Journal of Molecular Structure 994 (2011) 350–359

Contents lists available at ScienceDirect

Journal of Molecular Structure

journal homepage: www.elsevier.com/locate/molstruc

Structural (X-ray), spectral (FT-IR and Raman) and quantum chemical investigations of a series of 6-benzylaminopurine derivatives

Michal Čajan [a], Zdeněk Trávníček [b,*]

[a] Department of Inorganic Chemistry, Faculty of Science, Palacký University, 17. listopadu 12, CZ-771 47 Olomouc, Czech Republic
[b] Regional Centre of Advanced Technologies and Materials, Department of Inorganic Chemistry, Faculty of Science, Palacký University, 17. listopadu 12, CZ-771 46 Olomouc, Czech Republic

ARTICLE INFO

Article history:
Received 11 October 2010
Received in revised form 21 March 2011
Accepted 21 March 2011
Available online 25 March 2011

Keywords:
X-ray structure
Purine derivatives
Adenine derivatives
Vibrational spectra
Quantum chemical calculations

ABSTRACT

The structural and spectroscopic properties of 6-(2-methylbenzylamino)purine **1**, 6-(4-methylbenzylamino)purine **2**, 6-(3,4-dimethoxybenzylamino)purine **3**, 2-chloro-6-(3-bromobenzylamino)-9-isopropylpurine **4** and 2-chloro-6-(3,4-dichlorobenzylamino)-9-isopropylpurine **5** have been investigated by means of single crystal X-ray diffraction analysis, FT-IR and Raman spectroscopy, and quantum chemical calculations, where HF, DFT, RI-MP2 and MP2 methods in combination with the cc-pVDZ basis set have been used. The theoretically obtained structural as well as spectral parameters have been compared with those experimentally obtained. One of the unusual structural features is the finding that the electroneutral form of 6-(2-methylbenzylamino)purine **1** is protonated at the N7 position of the purine ring, which is not a typical protonation site for N9-unsubstituted adenine derivatives.

1. Introduction

6-Benzylaminopurine (*Bap*) derivatives represent heterocyclic compounds showing a large scale of biological activities. As the plant growth hormones, called cytokinins, they have been intensively studied since the 1960s. The key role of the cytokinins lies principally in participation in the controlling of the processes related to plant cell division and senescence [1–6]. It has been found that the appropriate structural modification of the *Bap* molecule can lead to a substantial change of its biological and physiological properties. Thus, *Bap* derivatives substituted at the C2 and N9 positions of the purine moiety show the inhibition activity against cyclin-dependent kinases (CDKs) [7–9], and some of them (e.g. *olomoucine* = 6-(benzylamino)-2-[(2-hydroxyethyl)amino]-9-methylpurine, *bohemine* = 6-(benzylamino)-2-[(3-hydroxypropyl)-amino]-9-isopropylpurine, *roscovitine* = 6-(benzylamino)-2-[(1-hydroxymethyl-propyl)amino]-9-isopropylpurine also show significant both *in vitro* and *in vivo* cytotoxicity against some human cancer cell lines [10–12]. Except for the above-mentioned organic skeleton derivatization, the resulting cytotoxicity may be also increased after complex formation of such heterocyclic compounds with suitable transition metals, like Fe, Co, Pt, Pd, Cu, etc. To date, many of these metal complexes have been extensively studied owing to their possible medical application as enzyme inhibitors [13], antiviral [14], anti-bacterial [15], and anti-cancer agents [16,17].

Coordination abilities as well as physiological activity of both cytokinins and CDK inhibitors are strongly influenced by molecular geometry, electron density distribution within the appropriate molecule, and finally by possible tautomeric equilibria related to the proton position at the unsubstituted nitrogen atoms of the purine ring. Thus, this work is devoted to the detailed analysis of structural and spectroscopic properties within two structurally different types of 6-benzylaminopurine derivatives, i.e. 6-(2-methylbenzylamino)purine **1**, 6-(4-methylbenzylamino)purine **2**, and 6-(3,4-dimethoxybenzylamino)purine **3** as the compounds with the unsubstituted imidazole moiety, and 2-chloro-6-(3-bromobenzylamino)-9-isopropylpurine **4** and 2-chloro-6-(3,4-dichlorobenzylamino)-9-isopropylpurine **5** as the second group of compounds, where the purine ring is modified by the chloro and isopropyl substituents at the C2, and N9 position, respectively.

Although the compounds **1** and **2** are chemically very similar, their molecular structures differ in the position of the hydrogen atom at the imidazole moiety of the purine ring. The molecule of **1** is protonated at the N7 position, while the compound **2** prefers protonation at the N9 position as is usual for most of similar purine systems of this type. To our best knowledge, only one electroneutral analog with the hydrogen atom positioned just at N7 has been prepared up to now [18]. All the compounds presented in this work were experimentally characterized by elemental analysis, FT-IR

* Corresponding author. Tel.: +420 585 634 352; fax: +420 585 634 954.
E-mail address: zdenek.travnicek@upol.cz (Z. Trávníček).

0022-2860/$ - see front matter © 2011 Elsevier B.V. All rights reserved.
doi:10.1016/j.molstruc.2011.03.049

and Raman measurements, and single crystal X-ray analysis. The experimentally found structural as well as spectroscopic data were compared with those obtained by quantum chemical calculations performed at the DFT, RI-MP2 and MP2 levels of theory.

2. Material and methods

2.1. Syntheses and characterizations

Compounds **1**–**3**: 6-Benzylaminopurine derivatives were prepared according to the well known synthetic strategy which is depicted in Scheme 2, i.e. by the reaction of 6-chloropurine with the appropriate R-substituted benzylamine and triethylamine (Et_3N) in the butanol solution, in a molar ratio of 3:4:5 [19]. The yields obtained were 70–80%. The single crystals of the discussed compounds were obtained by re-crystallization from *N*,*N*′-dimethylformamide.

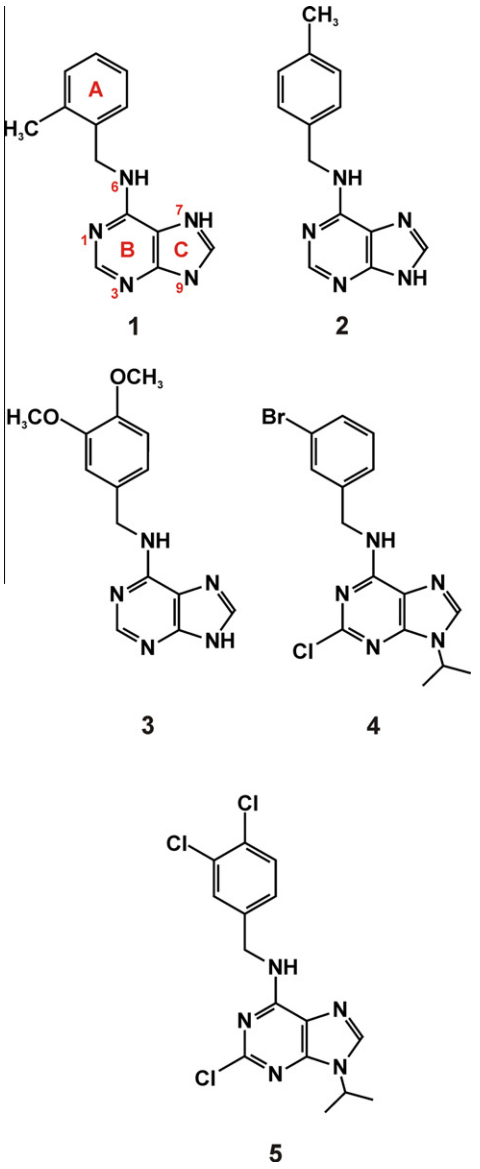

Scheme 1. Structural formulas of the studied compounds (6-(2-methylbenzylamino)purine **1**, 6-(4-methylbenzylamino)purine **2**, and 6-(3,4-dimethoxybenzylamino)purine **3**, 2-chloro-6-(3-bromobenzylamino)-9-isopropylpurine **4** and 2-chloro-6-(3,4-dichlorobenzylamino)-9-isopropylpurine **5**), showing the nitrogen atoms numbering and rings labeling (A – benzene, B – pyrimidine and C – imidazole).

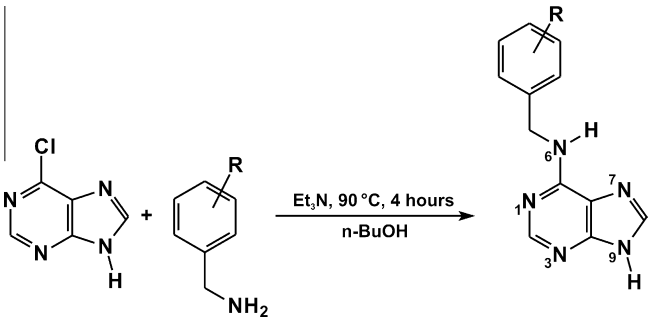

Scheme 2. A general pathway for the preparation of 6-benzylaminopurine derivatives (R: CH_3 or OCH_3).

Compounds **4** and **5**: 2,6-dichloro-9-isopropylpurine (L1) was prepared from 2,6-dichloropurine according to the previously reported general preparation of 2,6-dihalogen-9-alkylpurine derivatives [20]. The synthesis of **4** and **5** follows the published procedure of C2,N9-substituted 6-benzylaminopurine derivatives [21] (see Scheme 3), where a mixture of L1 and the corresponding benzylamine derivative (in a molar ratio of 1:1) was stirred in 150 ml of ethyl acetate at the temperature of 78 °C for 5 h. Then, the products were filtered off, washed with ethanol and diethyl ether, and dried at 40 °C. The yields ranged from 76% to 88%. The single crystals were prepared by slow evaporation of the isopropanol/acetone mixture (1:1) at laboratory temperature.

6-(2-Methylbenzylamino)purine **1** Yield: 77%. Anal. Calc. for $C_{13}N_5H_{13}$: C, 65.3; H, 5.5; N, 29.3. Found: C, 64.9; H, 5.5; N, 29.5%. *6-(4-Methylbenzylamino)purine* **2**. Yield: 80%. Anal. Calc. for $C_{13}N_5H_{13}$: C, 65.3; H, 5.5; N, 29.3. Found: C, 65.6; H, 5.3; N, 29.1%. *6-(3,4-Dimethoxybenzylamino)purine* **3**. Yield: 78%. Anal. Calc. for $C_{14}N_5O_2H_{15}$: C, 58.9; H, 5.3; N, 24.5. Found: C, 59.1; H, 5.2; N, 24.8%. *2-Chloro-6-(3-bromobenzylamino)-9-isopropylpurine* **4**. Yield: 73%. $C_{15}N_5ClBrH_{15}$: C, 47.3; H, 4.0; N, 18.4. Found: C, 47.6; H, 4.4; N, 18.4%. *2-Chloro-6-(3,4-dichlorobenzylamino)-9-isopropylpurine* **5**. Yield: 76%. Anal. Calc. for $C_{15}N_5Cl_3H_{14}$: C, 48.6; H, 3.8; N, 18.9. Found: C, 48.9; H, 3.8; N, 18.5%.

2.2. X-ray crystallography, FT-IR and Raman Spectroscopy

Diffraction data were collected on an Xcalibur™ 2 diffractometer (Oxford Diffraction, Ltd.) equipped with Sapphire2 CCD detector using Mo Kα radiation (monochromator Enhance, Oxford Diffraction, Ltd.) and ω-scan rotation techniques at 100 K. Data collection, cell parameter refinements and data reduction were performed with the CrysAlis software package (Version 1.171.33.52, Oxford Diffraction, Ltd., Abingdon, England, 2009). The structures were solved by direct methods and refined anisotropically on F^2 using full-matrix least-squares approach (SHELX-97 software package) [22]. Hydrogen atoms were found from Fourier maps and refined with the riding model [C—H distance of 0.95 and 0.98 Å, N—H distance of 0.88 Å, and with U_{iso}(H) values of $1.2U_{eq}$(CH, CH_2, NH) or $1.5U_{eq}$(CH_3)]. The molecular and crystal structures were drawn with Diamond 3.2d program [23], which was also used for interpretation of the additional structural parameters.

FT-IR spectra were measured on a Nexus 670 FT-IR spectrometer (ThermoNicolet) by the KBr pellets technique in the range of 400–4000 cm^{-1}. Raman spectra were measured in the range of 150–4000 cm^{-1} on a Nicolet NXR 9650 device with a liquid nitrogen cooled NXE Genie germanium detector (ThermoNicolet) using the laser line 1064 nm and laser power 1.002 W.

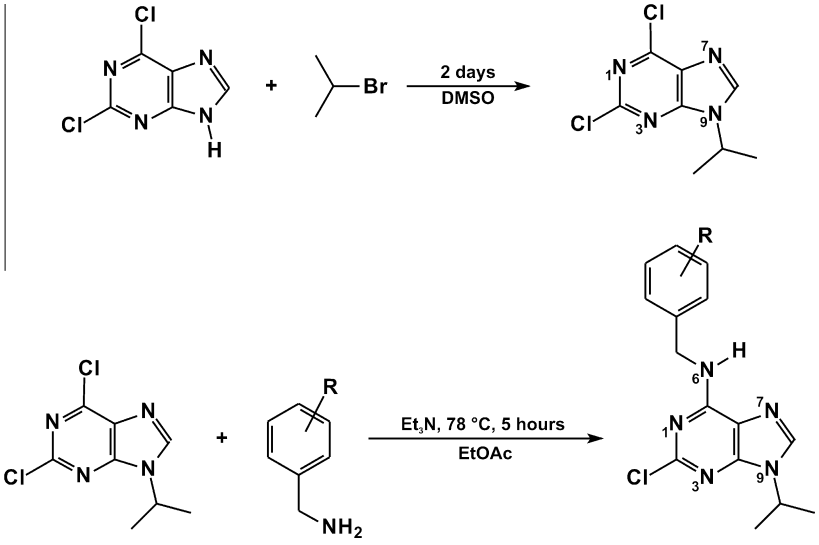

Scheme 3. A general pathway for the preparation of 2-chloro-6-benzylamino-9-isopropylpurine derivatives (R = Br or Cl).

2.3. Quantum chemical calculations

Geometries of the studied compounds as well as their infrared and Raman spectral properties were calculated at the DFT, RI-MP2 and MP2 levels. It is well known that HF and DFT do not often correctly describe the molecular structure, especially in the cases, when the geometry of a molecule is influenced by weak non-covalent intramolecular and intermolecular interactions [24], and thus, we decided to perform the geometry optimization also using the RI-MP2 and MP2 approaches with the aim to compare these results with those obtained by the non-correlated methods. In the RI-MP2 method, 4-center 2-electron integrals are approximated by 3-center 2-electron integrals using optimized auxiliary basis functions. This leads to an enormous speedup of the calculations and significant decreasing in memory requirements without the loss of accuracy when compared to the conventional MP2 method [25–27]. As input geometries, the geometries determined by single crystal X-ray analysis were used. DFT calculations were performed with a Gaussian 03 program [28] based on the B3LYP functional and the cc-pVDZ basis set. RI-MP2 and MP2 calculations, both also with the cc-pVDZ basis set were performed with a Turbomole 5.10 program [29]. Harmonic frequency analysis was used to verify the nature of determined stationary points as the minima as well as for the calculation of zero-point energies (ZPE). The calculated infrared frequencies were scaled by the 0.9084 factor in the case of HF, 0.9709 factor in the case of B3LYP, 0.9543 factor in the case of MP2 [30], and universal scaling factor of 0.9560 for the RI-MP2 approach [31].

3. Results and discussion

3.1. Structural analysis (X-ray crystallographic and QM study)

The molecular structures of the compounds **1**–**5** together with the atom numbering scheme are shown in Figs. 1 and 2. Crystal data and structure refinements are given in Table 1, selected bond lengths and angles together with the corresponding quantum chemical data obtained at the HF, DFT, RI-MP2 and MP2 levels are summarized in Table 2.

Although the prepared *Bap* derivatives are structurally very similar within both the studied groups, i.e. compounds **1**–**3** versus **4** and **5**, the subtituent's type and its position on the phenyl group lead to significant differences in the solid state molecular as well as crystal structure. In the group of derivatives with the unsubstituted pyrimidine and imidazole moieties, i.e. the compounds **1**–**3**, the compound **1** crystallizes in the $P2_1/c$ space group, while **2** as well as **3** in the $P\bar{1}$ space group. The purine rings of both compounds **4** and **5** are modified by the chloro and isopropyl substituents at the C2, and N9 position, respectively. Concerning their crystal structures, compound **4** crystallizes in $P\bar{1}$ while compound **5** in the $P2_1/c$ space group.

Each of the molecules investigated contains nearly planar benzene (A), pyrimidine (B) and imidazole (C) ring systems (Scheme 1). Maximum deviations from ring planarity were experimentally determined as follows: compound **1**: −0.0052(14) Å for C13 (ring A), 0.0095(13) Å for C6 (ring B) and −0.0012(13) Å for C4 (ring C); compound **2**: −0.0029(14) Å for C10 (ring A), −0.0077(14) Å for C4 (ring B) and −0.0025(14) Å for C8 (ring C); and compound **3**: −0.0039(13) Å for C10 (ring A), 0.0194(13) Å for C4 (ring B) and 0.0055(13) Å for C8 (ring C). The pyrimidine (B) and imidazole (C) rings in the molecules of **1** and **2** are nearly coplanar, making the dihedral angle of 2.10(4)° for **1** and 1.37(5)° for **2**. In the case of compound **3**, the purine system is more deformed and the experimental value of the mentioned dihedral angle was found to be 4.37(4)°. The dihedral angles between the benzene and purine planes are quite different, i.e. 67.14(4)° for **1**, 80.34(4)° for **2**, and 88.73(3)° for **3**. The torsion angles between the bonds connecting benzene and purine planes are 173.95(12)° for **1**, −78.48(15)° for **2**, and −98.2(1)° for **3** in the case of the C6—N6—C9—C10 angle, and 114.06(13)° for **1**, −67.58(16)° for **2**, and 1.2(2)° for **3** in the case of the N6—C9—C10—C15 one. Concerning the second group of the compounds, the maximum deviations from rings planarity have been determined as follows: compound **4**: 0.006(2) Å for C13 (ring A), 0.012(2) Å for C6 (ring B), and 0.006(2) Å for C4 (ring C); compound **5**: −0.008(2) Å for C11 (ring A), 0.011(2) Å for C6 (ring B) and 0.0029(15) Å for C4 (ring C). The pyrimidine (B) and imidazole (C) rings are in fact coplanar, with the dihedral angle of 0.71(7)° for **4** and 0.95(5)° for **5**. The dihedral angles between the benzene and purine planes are 76.78(6)° for **4**, and 80.34(4)° for **2**. The values of the related torsion angles have been found to be 126.7(2)° for **4** and 105.4(2)° for **5** in the case of the C6—N6—C9—C10 angle, and −146.2(2)° for **4**, and −47.6(2)° for **5** in the case of the N6—C9—C10—C15 one.

Regarding the crystal structure description, the compounds **1** and **2** are substituted only by the methyl group at the phenyl ring.

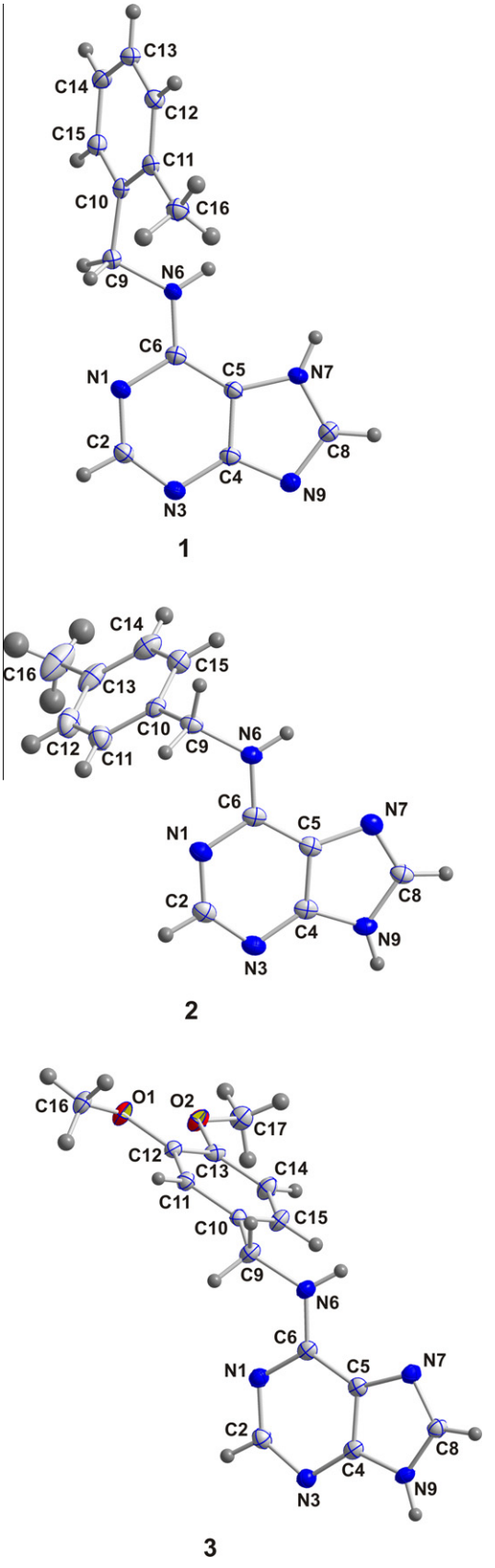

Fig. 1. The molecular structures of compounds **1**, **2** and **3** together with the atom numbering scheme. Non-hydrogen atoms are drawn as thermal ellipsoids at the 50% probability level.

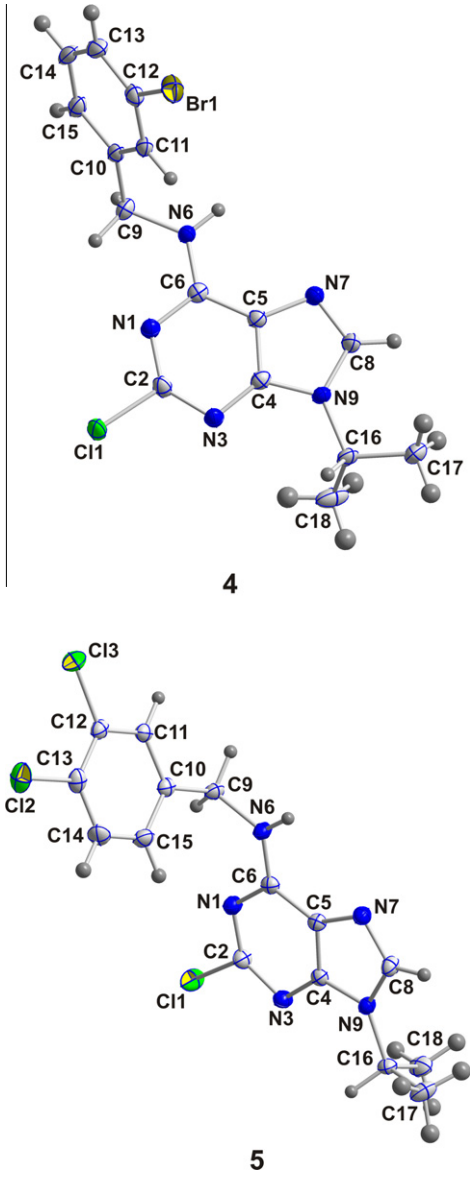

Fig. 2. The molecular structures of compounds **4** and **5** together with the atom numbering scheme. Non-hydrogen atoms are drawn as thermal ellipsoids at the 50% probability level.

In this case, the secondary structure is stabilized by intermolecular hydrogen bonds of the N—H···N type (N6—H···N9 and N7—H···N3 for **1**, N6—H···N7 and N9—H···N3 for **2**, for details see Fig. 4), and other non-covalent interactions of the C—H···N and C—H···C types. The molecules of the compounds **3**–**5** contain also the oxygen, chlorine and bromine atoms. Thus, besides N—H···N hydrogen bonds (N6—H···N7 and N9—H···N3 for **3** and N6—H···N7 for **4** and **5**) and C—H···N and C—H···C interactions, their secondary structures are additionally formed by several C—H···X weak non-covalent interactions of the van der Waals type, where X stands for the O atom in CH_3O (**3**), Br atoms in **4** and Cl atom in **5**.

In the case of the compounds **1**–**3**, the above-mentioned N—H···N hydrogen bonds arrange the molecules into infinite 1D chains (Fig. 3), with the N···N distances ranging from 2.834 to 3.035 Å (for more detailed information see Supplementary material). It was observed that the N3···N9 and N3···N7 distances are generally shorter by approximately 0.1 Å in comparison with those

Table 1
Crystal data and structure refinements for 6-(2-methylbenzylamino)purine **1**, 6-(4-methylbenzylamino)purine **2**, and 6-(3,4-dimethoxybenzylamino)purine **3**, 2-chloro-6-(3-bromobenzylamino)-9-isopropylpurine **4** and 2-chloro-6-(3,4-dichlorobenzylamino)-9-isopropylpurine **5**.

	1	**2**	**3**	**4**	**5**
Empirical formula	$C_{13}N_5H_{13}$	$C_{13}N_5H_{13}$	$C_{14}N_5O_2H_{15}$	$C_{15}H_{15}BrClN_5$	$C_{15}H_{14}Cl_3N_5$
Formula weight	239.28	239.28	285.31	380.68	370.66
Crystal system	Monoclinic	Triclinic	Triclinic	Triclinic	Monoclinic
Space group	$P2_1/c$	$P\bar{1}$	$P\bar{1}$	$P\bar{1}$	$P2_1/c$
Unit cell dimensions					
a (Å)	9.2557(3)	4.8792(2)	7.5546(3)	7.1968(2)	12.7552(2)
b (Å)	11.2039(3)	8.0596(3)	8.3225(3)	10.3372(3)	9.58947(12)
c (Å)	11.3211(4)	15.1224(6)	10.3124(4)	11.6119(3)	14.1985(3)
α (°)	90.00	88.983(3)	85.698(3)	96.480(2)	90.00
β (°)	100.550(4)	82.091(4)	87.665(3)	101.680(2)	110.387(2)
γ (°)	90.00	80.131(3)	88.714(3)	108.128(2)	90.00
Z	4	2	2	2	4
V (Å^3)	1154.15(7)	580.29(4)	645.89(4)	789.51(3)	1627.90(5)
$D_{calc.}$ (g cm^{-3})	1.377	1.369	1.467	1.601	1.512
T (K)	100(2)	100(2)	105(2)	108(2)	110(2)
μ (mm^{-1})	0.089	0.088	0.103	2.776	0.568
T_{max}/T_{min}	0.9782 / 0.9739	0.9826/0.9741	0.9648/0.9599	0.6067/0.4897	0.8480/0.8046
Index ranges	$-11 \leqslant h \leqslant 10$ $-11 \leqslant k \leqslant 13$ $-13 \leqslant l \leqslant 13$	$-5 \leqslant h \leqslant 5$ $-9 \leqslant k \leqslant 7$ $-17 \leqslant l \leqslant 17$	$-8 \leqslant h \leqslant 8$ $-8 \leqslant k \leqslant 9$ $-12 \leqslant l \leqslant 12$	$-8 \leqslant h \leqslant 8$ $-8 \leqslant k \leqslant 12$ $-13 \leqslant l \leqslant 13$	$-15 \leqslant h \leqslant 15$ $-11 \leqslant k \leqslant 11$ $-16 \leqslant l \leqslant 16$
θ Range (°) for data collection	$3.19 \leqslant \theta \leqslant 25.00$	$2.91 \leqslant \theta \leqslant 25.00$	$3.04 \leqslant \theta \leqslant 25.00$	$3.04 \leqslant \theta \leqslant 25.00$	$3.06 \leqslant \theta \leqslant 25.00$
Reflection collected/unique	8956/2020	3973/1956	5378/2261	5350/2785	13711/2867
R_{int}	0.0343	0.0227	0.0214	0.0156	0.0105
Data/restrains/parameters	2020/0/164	1956/0/164	2261/0/192	2785/0/201	2867/0/210
Goodness-of-fit on F^2	1.043	1.013	1.105	1.101	1.097
Final R indices [$I > 2\sigma(I)$]	R1 = 0.0343 $wR2$ = 0.0889	R1 = 0.0355 $wR2$ = 0.0918	R1 = 0.0328 $wR2$ = 0.0944	R1 = 0.0280 $wR2$ = 0.0736	R1 = 0.0286 $wR2$ = 0.0827
R indices (all data)	R1 = 0.0463 $wR2$ = 0.0927	R1 = 0.0468 $wR2$ = 0.0961	R1 = 0.0377 $wR2$ = 0.0996	R1 = 0.0301 $wR2$ = 0.0747	R1 = 0.0312 $wR2$ = 0.0845
Largest peak and hole (e Å^{-3})	0.182 and −0.204	0.194 and −0.151	0.208 and −0.182	0.619 and −0.606	0.512 and −0.263

Table 2
Selected geometric parameters (bond lengths in Å, and angles in °) of compounds **1–5** as determined by single crystal X-ray analysis and various quantum-chemical methods (all with the cc-pVDZ basis set).

	Method	N1—C2	N1—C6	C2—N3	N3—C4	C5—C6	N7—C5	N7—C8	N9—C4	N9—C8	C2—N1—C6	C2—N3—C4	C5—N7—C8	C4—N9—C8
1	X-ray	1.337(2)	1.351(2)	1.328(2)	1.356(2)	1.410(2)	1.383(2)	1.338(2)	1.377(2)	1.324(2)	118.51(11)	112.10(11)	106.28(10)	103.36(10)
	HF	1.3398	1.3162	1.3041	1.3366	1.3996	1.3851	1.3539	1.3737	1.2899	118.49	113.28	105.26	104.57
	B3LYP	1.3530	1.3377	1.3278	1.3483	1.4102	1.3863	1.3762	1.3848	1.3122	118.31	112.94	105.92	104.48
	RI-MP2	1.3664	1.3369	1.3341	1.3551	1.4143	1.3748	1.3832	1.3869	1.3229	117.94	112.70	106.12	103.95
	MP2	1.3647	1.3352	1.3341	1.3541	1.4137	1.3747	1.3833	1.3862	1.3214	118.07	112.69	106.08	103.99
2	X-ray	1.333(2)	1.356(2)	1.335(2)	1.349(2)	1.407(2)	1.392(2)	1.311(2)	1.368(2)	1.362(2)	118.35(12)	110.48(12)	103.29(12)	105.98(12)
	HF	1.3321	1.3292	1.3124	1.3323	1.4071	1.3835	1.2827	1.3628	1.3717	118.64	111.26	104.13	106.45
	B3LYP	1.3465	1.3479	1.3368	1.3422	1.4170	1.3854	1.3138	1.3785	1.3816	118.46	110.88	103.90	106.76
	RI-MP2	1.3581	1.3477	1.3428	1.3481	1.4184	1.3835	1.3328	1.3817	1.3761	118.16	110.36	102.98	106.82
	MP2	1.3573	1.3472	1.3416	1.3472	1.4179	1.3819	1.3325	1.3791	1.3748	118.21	110.45	103.02	106.91
3	X-ray	1.337(2)	1.352(2)	1.334(2)	1.352(2)	1.406(2)	1.388(2)	1.315(2)	1.367(2)	1.361(2)	117.95(12)	110.93(11)	103.65(11)	106.42(11)
	HF	1.3322	1.3275	1.3127	1.3315	1.4064	1.3835	1.2828	1.3632	1.3715	118.58	111.34	104.13	106.43
	B3LYP	1.3459	1.3469	1.3374	1.3420	1.4171	1.3855	1.3139	1.3789	1.3815	118.43	110.88	103.90	106.76
	RI-MP2	1.3583	1.3468	1.3428	1.3477	1.4186	1.3836	1.3324	1.3808	1.3759	118.11	110.36	102.99	106.87
	MP2	1.3571	1.3470	1.3419	1.3473	1.4170	1.3830	1.3319	1.3807	1.3746	118.17	110.37	103.00	106.82
4	X-ray	1.325(3)	1.347(3)	1.318(3)	1.348(3)	1.410(3)	1.387(3)	1.317(3)	1.370(3)	1.364(3)	117.6(2)	109.4(2)	103.5(2)	105.6(2)
	HF	1.3214	1.3298	1.3017	1.3360	1.4050	1.3792	1.2848	1.3613	1.3744	117.93	111.11	103.85	105.24
	B3LYP	1.3340	1.3478	1.3253	1.3452	1.4165	1.3820	1.3162	1.3783	1.3854	117.84	110.52	103.71	105.53
	RI-MP2	1.3475	1.3480	1.3340	1.3522	1.4196	1.3793	1.3374	1.3795	1.3800	117.54	109.72	102.86	105.76
	MP2	1.3480	1.3473	1.3323	1.3499	1.4167	1.3774	1.3368	1.3792	1.3791	117.77	109.85	102.94	105.73
5	X-ray	1.326(2)	1.350(2)	1.325(2)	1.351(2)	1.415(2)	1.383(2)	1.314(2)	1.373(2)	1.366(2)	117.61(13)	109.25(12)	103.47(12)	105.44(12)
	HF	1.3222	1.3310	1.3006	1.3367	1.4045	1.3789	1.2850	1.3606	1.3745	117.95	111.12	103.83	105.26
	B3LYP	1.3359	1.3492	1.3240	1.3457	1.4156	1.3816	1.3163	1.3777	1.3853	117.81	110.63	103.69	105.52
	RI-MP2	1.3486	1.3488	1.3339	1.3516	1.4184	1.3778	1.3370	1.3788	1.3799	117.69	109.83	102.89	105.72
	MP2	1.3477	1.3475	1.3322	1.3510	1.4174	1.3768	1.3362	1.3780	1.3790	117.73	109.85	102.92	105.74

of N7···N6 or N9···N6. The crystal structures of both the compounds **4** and **5** are formed by centrosymmetric dimers connected through the N6—H···N7 hydrogen bonds, where N···N interaction distances were found to be 3.012(3) Å for **4** and 2.975(2) Å for **5**. All the discussed non-covalent interactions as well as their symmetry codes are summarized in Tables S1–S5 and Figs. S1 and S2 in Appendix A: Supplementary material section. The above-mentioned nonbonding interactions within the crystal structures resulted in significant differences in dihedral angles between benzene and purine rings as well as in the C6—N6—C9—C10 and

N6—C9—C10—C15 torsion angles, as has been discussed above. For the same reason, the used theoretical approaches have provided more or less different values. Comparable results have been obtained only in the case of the RI-MP2 and MP2 levels, which well confirm the profitability of the resolution identity approximation. Quantitative agreement between the experimental and theoretical results is observable only in the case of the compound **1**, as it is evident from Table 3.

Proton positioning at the N7 atom of the compound **1** leads to significant geometric changes compared to the N9-protonated as well as N9-substituted derivatives, particularly at the imidazole part of the purine ring. The found differences are generally caused by the hybridization type of the corresponding nitrogen atom, which is specifically sp^2 for the unsubstituted and sp^3 for the substituted/protonated one. Thus, the apparent differences between the N7-protonated compound **1** and N9-substituted/protonated compounds **2**–**5** have been found for the N9—C8 and N7—C8 bond lengths, and principally for the C5—N7—C8 and C4—N9—C8 internal angles (see Table 2). The C—N bonds formed by protonated nitrogen have been found longer by 0.014 Å for **1**, and 0.051 and 0.046 Å for **2**, and **3**, respectively. Similarly, nitrogen substitution leads to the C—N—C internal angle value typically higher by approximately 3.0° in comparison with the unprotonated system.

Thus, the experimental bond distances are 1.324(2) Å (**1**), 1.362(2) Å (**2**), 1.361(2) Å (**3**), 1.364(3) Å (**4**), and 1.366(2) Å (**5**) for the N9—C8 bond length; 1.338(2) Å (**1**), 1.311(2) Å (**2**), 1.315(2) Å (**3**), 1.317(3) Å (**4**), 1.314(2) Å (**5**) for the N7—C8 bond length. The experimental values of the internal angle C4—N9—C8 are 103.36(10)° for **1**, 105.98(12)° for **2**, 106.42(11)° for **3**, and 105.6(2)° for **4**, 105.44(12)° for **5**. The values of the internal angle C5—N7—C8 are 106.28(10)° for **1**, 103.29(12)° for **2,** 103.65(11)° for **3**, 103.5(2)° for **4**, 103.47(12)° for **5**. The values obtained by the MP2/cc-pVDZ approach (as the most accurate from those used) are rather similar, i.e. 1.3214 Å (**1**), 1.3748 Å (**2**), 1.3746 Å (**3**), 1.3791 Å (**4**), and 1.3790 Å (**5**) for the N9—C8 bond length, and 1.3833 Å (**1**), 1.3325 Å (**2**), 1.3319 Å (**3**), 1.3368 Å (**4**), and 1.3362 Å (**5**) for the N7—C8 bond length. Also in this case, bond lengths calculated for protonated nitrogen are longer by approximately 0.05 Å. The values of internal angles calculated at the same level are 103.99° (**1**), 106.91° (**2**), 106.82° (**3**), 105.73° (**4**), and 105.74° (**5**) for the C4—N9—C8 angle, and 106.08° (**1**), 103.02° (**2**), 103.00° (**3**), 102.94° (**4**), and 105.74° (**5**) for the C5—N7—C8 angle.

In general, the accuracy of the calculated bond lengths is comparable in the whole range of the methods used. The deviations from the experimental crystallographic values do not exceed 0.05 Å. The calculated values of the key bond angles at the purine ring correspond much better with those obtained by X-ray analysis, where the deviations of the values obtained by both MP2 methods does not exceed 1.0°. As can be evident from Table 2, the best accuracy has been achieved at the RI-MP2 and MP2 levels as expected.

3.2. FT-IR and Raman spectroscopy

All the FT-IR as well as Raman spectra measured are presented in Figs. S3–S8 in Appendix A: Supplementary material section. Selected maxima observed in the experimentally measured FT-IR spectra and their assignments are presented in Table 4.

Due to the structural similarity of the studied compounds, several common characteristic features should be found, specifically in the purine and phenyl parts of the molecules. Most of the bands observable within the 640–900 cm^{-1} region originate from the purine skeletal vibrations. Similarly, the medium or strong intense peaks observed at 1460–1598 cm^{-1} belong to the $\nu(C{=}C)_{aromatic}$ skeletal vibrations of the both phenyl and purine moieties, while absorptions with strong intensity at 1619–1633 cm^{-1} belong to $\nu(C{=}N)_{aromatic}$ purine skeletal vibrations. The letter mentioned maxima reflect on similarity within the group of the studied compounds (see Fig. 3). The regions at 2800–3000 cm^{-1} and 3050–3135 cm^{-1} relate to the $\nu(C_{aliphatic}{-}H)$, and $\nu(C_{aromatic}{-}H)$ valence vibrations, respectively. The bands of weak or medium intensities observable within the 3258–3286 cm^{-1} and 3424–3430 cm^{-1} regions should be classified as the ν(N9(7)—H), and ν(N6—H) vibrations, respectively [32,33].

Other typical bands should be observed in dependence on structural differences of each individual studied compound. Thus, the strong maximum at 1268 cm^{-1} in the spectrum of **3** have been assigned to the $\nu(C_{phenyl}{-}O)$ vibration. The weak or medium maxima found at 668 and 1155 cm^{-1}, and observable only in the spectra of **4** and **5**, originate from the $\nu(C_{phenyl}{-}Br)$ vibration, and $\nu(C_{phenyl}{-}Cl)$ vibration, respectively.

The calculated frequencies enable more detailed analysis of the FT-IR spectra measured. Important vibrational frequencies obtained at the HF, B3LYP, RI-MP2 and MP2 levels of theory are summarized in Table 4. Generally speaking, all the methods used have given slightly overestimated frequency values in most cases. Such results should be undoubtedly assigned partly to the methodology errors, partly to the crystal field effects neglected. The frequencies of the $\nu(C{=}C)_{aromatic}$ vibrations of the benzene and purine moieties have been found overestimated by approximately 100 cm^{-1}, and the best results have been obtained at the B3LYP level (in the range of 1560–1619 cm^{-1}). Surprisingly, both RI-MP2 and MP2 approaches have provided worse results in this case. Regarding the intensity of signals, the evident correspondence between experimental and theoretical data has not been found for any calculation approach used. Where experimental values are rather medium intense, the HF as well as B3LYP approaches has also provided peaks of strong or very strong intensities. Both the RI-MP2 and MP2 calculations have contrariwise led to absorptions with very low

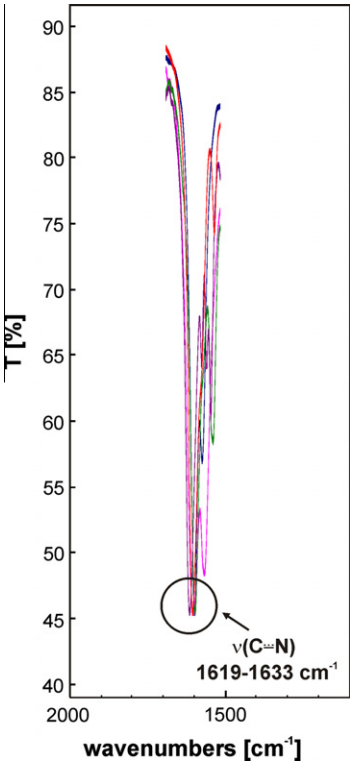

Fig. 3. Superposition of the maxima belonging to ν(C—N), showing on the similarity within the group of the studied compound **1**–**5**.

intensities. However, it must be said, that it is relatively difficult to separate the $\nu(C{=}C)_{aromatic}$ and $\nu(C{=}N)_{aromatic}$ skeletal vibrations within the purine moiety.

The $\nu(C{=}N)_{aromatic}$ skeleton vibrations of mostly strong or medium intensities have been found within the region of 1518–1663 cm^{-1} for HF, 1468–1596 cm^{-1} for B3LYP, for 1512–1688 cm^{-1} RI-MP2 and 1493–1688 cm^{-1} for MP2 approach. As it is evident from Table 4, their values are not significantly influenced by the substitution of the purine ring. The best agreement with experimental results has been found for both MP2 approaches.

Similarly, the $\nu(C_{aromatic}{-}H)$ vibrations have been found within the region of 3020–3079 cm^{-1} for HF, 3063–3122 cm^{-1} for B3LYP, 3038–3124 cm^{-1} for RI-MP2 and 3059–3126 cm^{-1} for the MP2 method, which has provided the best results. Majority of the values found are of weak intensity (contrary to experimental medium values). The band of weak intensity observable at 3096–3106 cm^{-1}

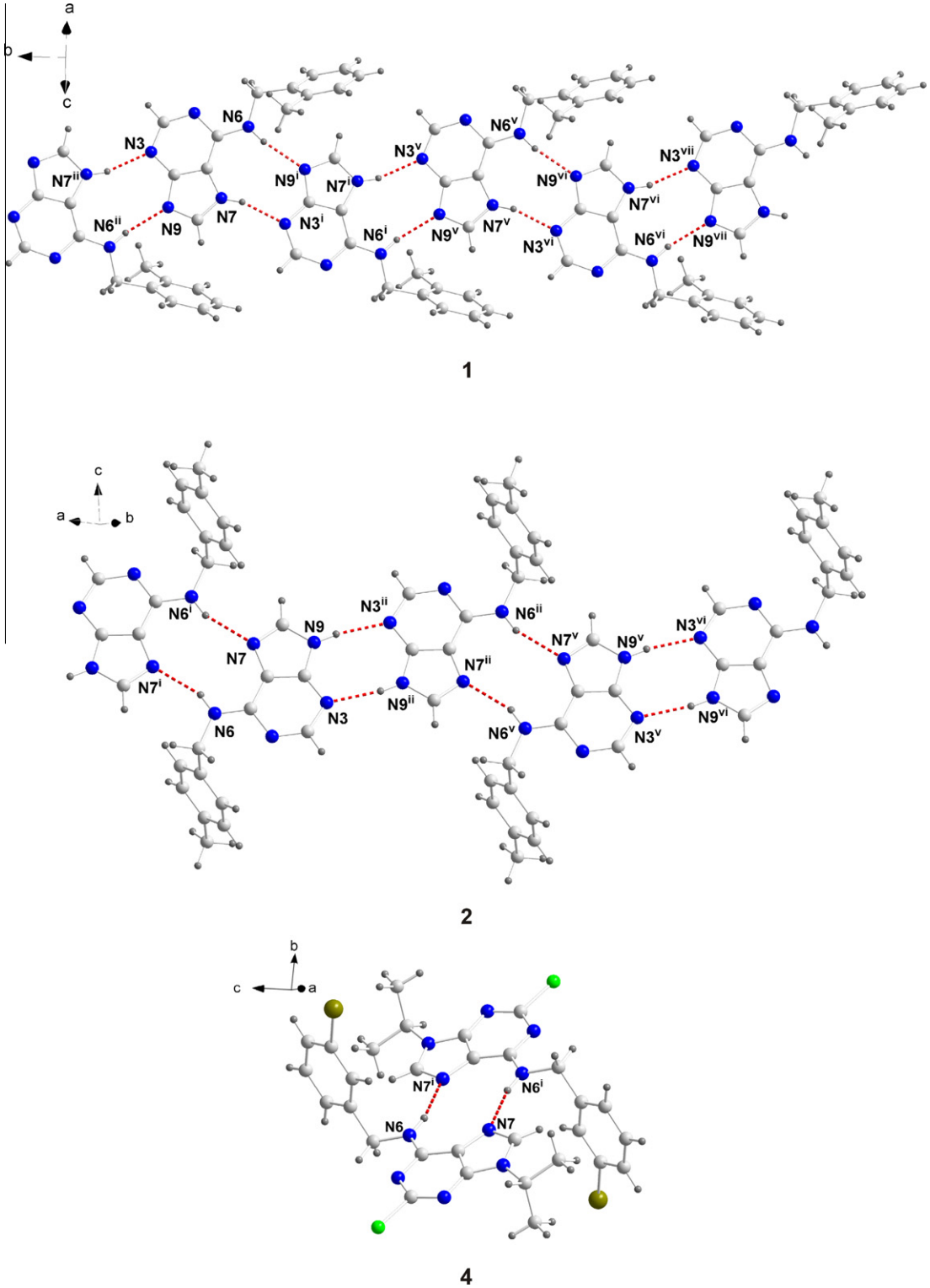

Fig. 4. Parts of the crystal structures of compounds **1**, **2** and **4**, showing the N—H···N hydrogen bonds (dashed lines), and depicting the formation of infinite one-dimensional chains of **1** and **2**, and centrosymmetric dimers (for **4**).

Table 3
Selected torsion angles (°) of compounds **1–5** determined by single crystal X-ray analysis and various quantum-chemical methods (all with the cc-pVDZ basis set).

Method	C6—N6—C9—C10					N6—C9—C10—C15				
	1	**2**	**3**	**4**	**5**	**1**	**2**	**3**	**4**	**5**
X-ray	173.95(12)	−78.4(2)	−98.2(2)	126.7(2)	105.4(2)	114.06(13)	−67.6(2)	1.2(2)	146.2(2)	−47.6(2)
HF	179.28	−101.33	−162.13	157.40	90.46	102.31	−109.87	46.21	128.34	−82.49
B3LYP	176.12	−100.26	−136.93	132.25	92.88	105.29	−109.52	40.27	143.44	−75.57
RI-MP2	177.83	−81.77	−77.34	75.46	73.24	104.54	−95.62	89.30	88.74	−90.94
MP2	178.05	−82.26	−77.79	75.72	73.44	104.48	−96.33	88.87	89.03	−90.76

Table 4
Selected experimental and calculated (all with the cc-pVDZ basis set) FT-IR vibration frequencies (cm^{-1}) of compounds **1–5** and their assignments.

Method	Comp.	ν(C=C)$_{aromatic}$	ν(C=N)$_{aromatic}$	ν(C$_{aromatic}$—H)	ν(C8—H)	ν(N$_{purine}$—H)	ν(N6—H)	ν(C$_{phenyl}$—X)	ν(C$_{purine}$—Cl)
Exp.	**1**	1565m, 1530w, 1460m	1625vs	3113m, 3050m		3262m	3427m		
	2	1598s, 1516w, 1460m	1620vs	3100m, 3062m		3258m	3426m		
	3	1592m, 1515s, 1487w	1623vs	3133m, 3071m		3286m	3430w	1268s[a]	
	4	1568s, 1536m, 1472m	1619vs	3132m, 3073m			3429w	668m[b]	
	5	1574m, 1539m, 1492m	1633vs	3129m, 3074m			3424w	1155m[c]	
HF	**1**	1641w, 1610w	1663s, 1551m, 1518s	3059–3024w/m	3096w	3548m	3478w		
	2	1645s, 1605w	1653s, 1569w, 1534s	3050–3020w	3102w	3538m	3499m		
	3	1646s, 1622m	1652s, 1565m, 1526m	3077–3047w/m	3102w	3539m	3493m	1324s, 1258s[a]	
	4	1645vs, 1623s	1645vs, 1571w, 1521s	3077–3037w	3105w		3489m	660w[b]	937m
	5	1631vs, 1622s	1647s, 1573w, 1525s	3079–3057w	3106w		3500m	1020m[c]	961m
B3LYP	**1**	1618s, 1610w, 1582w	1555s, 1497m, 1469m	3105–3070w	3143w	3533m	3473w		
	2	1619w, 1613s, 1577w	1594s, 1516m, 1471s	3094–3063w/m	3149w	3530m	3495m		
	3	1614vs, 1609m, 1590w	1596s, 1516m, 1472s	3122–3067w/m	3148w	3530m	3496m	1266s, 1230s[a]	
	4	1612vs, 1598w, 1570m	1579s, 1517w, 1468s	3121–3080w	3152w		3493m	658w[b]	912m
	5	1610vs, 1591w, 1561w	1575s, 1518w, 1469w	3120–3100w	3153w		3499m	1010w[c]	906m
RI-MP2	**1**	1673m, 1637w	1685s, 1606s, 1545s	3103–3066w	3161w	3522m	3425w		
	2	1686m, 1628w	1688s, 1645s, 1540m	3103–3038w	3159w	3519m	3456m		
	3	1670w, 1640m	1687s, 1647s, 1512m	3124–3092w	3159w	3520m	3452m	1343s, 1317s[a]	
	4	1659w, 1630m	1679vs, 1610s, 1585s	3119–3068w	3171w		3461m	692w[b]	954m
	5	1662w, 1610m	1679vs, 1608s, 1585s	3120–3086w	3172w		3464m	1063w	957m
MP2	**1**	1675w, 1637w	1686s, 1606s, 1543s	3106–3068w	3163w	3522m	3429w		
	2	1687w, 1646m	1688s, 1587w, 1512s	3105–3059w	3161w	3520m	3459w		
	3	1671w, 1641m	1687s, 1646s, 1513s	3126–3094w	3161w	3521m	3455m	1344s, 1288s[a]	
	4	1660w, 1631m	1680vs, 1611s, 1493s	3122–3071w	3173w		3464m	692w[b]	953m
	5	1663w, 1610s	1679vs, 1612s, 1494s	3123–3087w	3175w		3466m	1062m[c]	956m

vs = Very strong, s = strong, m = medium, w = weak.
[a] ν(C$_{aromatic}$—O).
[b] ν(C$_{aromatic}$—Br).
[c] ν(C$_{aromatic}$—Cl).

(HF), 3143–3153 cm^{-1} (B3LYP), 3159–3172 cm^{-1} (RI-MP2), and 3163–3175 cm^{-1} (MP2), belongs to the ν(C8—H) vibration.

The ν(N6—H) vibration has been identified in the 3478–3500 cm^{-1} (HF), 3473–3499 cm^{-1} (B3LYP), 3425–3463 cm^{-1} (RI-MP2), and 3429–3466 cm^{-1} (MP2) regions. All the values are slightly overestimated compared to experimental data (3420–3429 cm^{-1}). Similarly to experimental observations, the vibration intensities have been found to be weak or medium.

A substantial difference between experimental and calculated frequency values has been observed for the ν(N9(7)—H) vibration of the compounds **1–3**. In this case, the frequency is more influenced by N7—H···N3 or N9—H···N3 hydrogen bonds formed between the neighboring purine moieties in the crystal structure (Fig. 4). Thus, all the calculated values of this vibration are generally shifted by approximately 300 cm^{-1} to higher wavenumbers due to neglecting all the intermolecular interactions during the calculations. Both RI-MP2 and MP2 methods have provided the same results (3519–3522 cm^{-1} and 3520–3522 cm^{-1}). The HF and B3LYP calculations have led to slightly higher values (3538–3548 cm^{-1} and 3530–3533 cm^{-1}, contrary to the experimentally determined value of 3260 cm^{-1}).

As has been discussed above, molecules of compounds **1–3** are connected together via the N6—H···N9 and N7—H···N3 (for **1**) or N6—H···N7 and N9—H···N3 (for **2** and **3**) hydrogen bonds to form infinite 1D chains in the crystal structures, while molecules of compounds **4** and **5** have been found to be arranged as

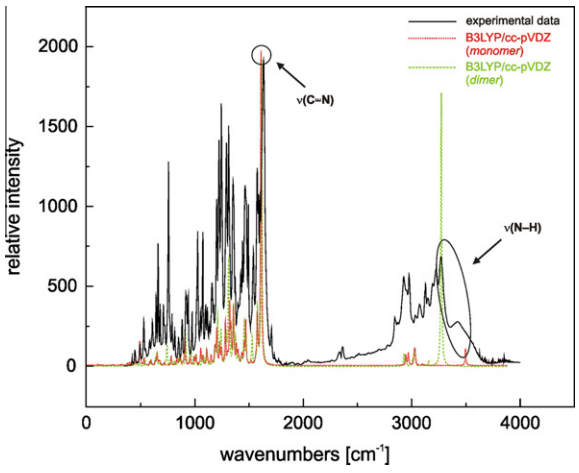

Fig. 5. Superposition of the experimentally measured (black line) and calculated FT-IR spectra for compound **5** (dotted line for isolated monomer, dashed line for centrosymmetric dimer), showing the influence of N—H···N hydrogen bonds on the ν(N—H) and (C—N) vibrational maxima.

Table 5
Selected Raman spectral data (cm^{-1}) of compounds **1**–**5** and their assignments.

Method	Comp.	$\nu(C{=}C)_{aromatic}$	$\nu(C{=}N)_{aromatic}$	$\nu(C_{aromatic}{-}H)$	$\nu(C_{aliphatic}{-}H)$	$\nu(C{-}X)$
Exp.	**1**	1568w, 1493w, 1461w	1604w	3113w, 3048w	3000w, 2925w, 2880w	
	2	1562w, 1489w, 1452w	1610w	3130w, 3055w	3009w, 2912w, 2919w	
	3	1532w, 1460w,	1595m	3133w, 3082w, 3055w	3003w, 2937w, 2835w	
	4	1573w, 1534w, 1478m	1592w	3142w, 3072w, 3053w	2981m, 2930m, 2868w	1164w
	5	1571m, 1532w, 1474m	1596w	3132w, 3074w, 3057m	2985w, 2929m, 2872w	1167w

X = Cl, Br.
vs = Very strong, s = strong, m = medium, w = weak.

centrosymmetric dimers connected thorough the N6—H···N7 hydrogen bonds. Thus, the comparative HF, DFT and RI-MP2 calculations have been performed for the systems of compounds **2**, **4** and **5**, with aim to investigate the influence of the above-mentioned hydrogen bonds on the values of calculated infrared frequencies. Significant differences have been found for the ν(N9—H) and ν(N6—H) vibrations, which values are generally shifted to lower wavenumbers and are also very close to the experimentally determined ones. Superposition of experimental and calculated spectra of compound **5** is shown in Fig. 5 Selected maxima calculated for these "dimers" and their comparison with results obtained for isolated molecules are presented in Table S6 in Appendix A: Supplementary material section.

Concerning the $\nu(C_{phenyl}{-}O)$ vibrations of **3**, the wavenumbers 1266 and 1230 cm^{-1} obtained by the B3LYP approach represent the best agreement with the experimental values. The MP2, RI-MP2 and HF methods have generally provided values overestimated by 60–80 cm^{-1}. Two types of the ν(C—Cl) vibration expected in the spectra of the compounds **4** and **5** have been identified. The first one, which is located at higher wavenumbers belongs to the $\nu(C_{phenyl}{-}Cl)$ vibration. The MP2 approaches have led to the best agreement with the experimental value, when the calculated values are 1063 cm^{-1} for RI-MP2 and 1062 cm^{-1} for MP2. The second one corresponds to the $\nu(C_{purine}{-}Cl)$ vibration and has been found within the region of 953–957 cm^{-1} (also for both MP2 methods). The $\nu(C_{phenyl}{-}Br)$ vibration of **4** has been found at 692 cm^{-1} (MP2).

Selected maxima observed in Raman spectra and their assignments are summarized in Table 5. The maxima observed in the range of 842–889 cm^{-1} belong to the $\delta(C_{aromatic}{-}H)$ vibrations. The weak or medium maxima in the range of 1452–1573 cm^{-1} may be assigned to the $\nu(C{=}C)_{aromatic}$ vibration. The bands of weak or medium intensity found between 1592 and 1610 cm^{-1} relate to the $\nu(C{=}N)_{aromatic}$ vibration. The bands found at 2835–3009 cm^{-1} and 3048–3142 cm^{-1} belong to the $\nu(C_{aliphatic}{-}H)$, and $\nu(C_{aromatic}{-}H)$ vibration, respectively [34–36].

The intensities of the $\nu(C{=}C)_{aromatic}$ vibration range from weak to medium, while the $\nu(C{=}N)_{aromatic}$ vibration have been found to be generally weak. The $\nu(C_{aromatic}{-}H)$ vibration shows the medium or strong intensity, contrary to weak intensity observed in the infrared spectra. The ν(N6—H) Raman vibrations show medium intensity and are generally more intense than those from the infrared spectra. The ν(N9(7)—H) vibrations have been found to be strong intense. Compared with the experimentally measured spectra, both ν(N—H) vibrations show the activity in the calculated spectra only. This difference is also probably given by the presence of the N—H···N intermolecular hydrogen bonds, whose role has been neglected in the calculation. Finally, the ν(C—O), ν(C—Cl) and ν(C—Br) vibrations have been found to be weak, contrary to medium or strong intensities observed in the infrared spectra. Concerning the results obtained by RI-MP2 and MP2 methods, the Turbomole program package does not provide the Raman intensities, and thus these could not be discussed here.

4. Conclusions

In this work, we have investigated structural and vibrational properties of several 6-benzylaminopurine derivatives using a combination of single crystal X-ray diffraction analysis, FT-IR and Raman spectroscopy, and quantum chemical calculations. The studied compounds should be divided into two structurally different groups. The compounds **1**, **2** and **3** represent the derivatives with the unsubstituted imidazole moiety, while the compounds **4** and **5** have been additionally modified by the chloro and isopropyl substituents at the C2, and N9 position, respectively. Concerning the molecular structures of the studied compounds, the electroneutral form of **1** shows the non-typical protonation at the N7 position of the purine ring. The crystal structures of all the compounds are stabilized by the hydrogen bonds of the N—H···N type accompanied by several weak non-covalent interactions of the C—H···C and C—H···X (X = O, Cl, Br) types. The molecules of **1**, **2** and **3** form infinite 1D chains bound by hydrogen bonds, while compounds **4** and **5** form centrosymmetric dimers.

In general, the accuracy of the calculated bond lengths is comparable in the whole range of the methods used. The deviations from the experimental crystallographic values do not exceed 0.05 Å. The calculated values of the key bond angles at the purine ring correspond much better with those obtained by X-ray analysis, when the deviations of the obtained values do not exceed 1.0°.

In order to assign important molecular vibrations, the quantum chemical calculations of infrared as well as Raman spectra based on the HF, DFT, RI-MP2 and MP2 approaches were used. Generally speaking, both RI-MP2 and MP2 methods have provided results comparable with the experimental data, while the HF and DFT frequencies have been generally underestimated. Observed deviations are given partly due to the methodology errors, partly due to the crystal field effects neglecting. A substantial difference between the experimental and calculated frequency values has been observed only for the ν(N9(7)—H) and ν(N6—H) vibrations of the compounds. In these cases, the frequency is more influenced by hydrogen bonds formed between the neighboring purine moieties in the crystal structure. Similarly, the ν(N—H) vibrations have been found to be active only in the calculated Raman spectra if compared with those experimentally measured. Regarding the intensity of signals, the evident correspondence between experimental and theoretical data has not been generally found for any calculation approach used.

Acknowledgements

This research was supported by the Ministry of Education, Youth and Sports of the Czech Republic (MSM6198959218), Grant Agency of the Academy of Science of the Czech Republic (IAA401370901), and by the Operational Program Research and Development for Innovations – European Social Fund (CZ.1.05/2.1.00/03.0058). The authors would like to thank Mr. Lukáš Dvořák

for help with the preparation of some of the studied compounds and their single crystals.

Appendix A. Supplementary material

The hydrogen bonds and non-covalent interaction parameters of compounds **1**–**5**, the figures showing the crystal packing as well as FT-IR and Raman spectra of all the compounds studied are presented in the Supplementary material section. Crystallographic data for the structures of the compounds **1**–**5** have been deposited within the Cambridge Crystallographic Data Centre, 12 Union Road, Cambridge CB2 1EZ, UK; fax: +44 1223 336 033; email: deposit@ccdc.cam.ac.uk, or at http://www.ccdc.cam.ac.uk with the deposition numbers CCDC 794403–794407. These data can be obtained free of charge *via* www.ccdc.cam.ac.uk/data_request/cif. Supplementary data associated with this article can be found, in the online version, at doi:10.1016/j.molstruc.2011.03.049.

References

[1] F. Skoog, H.Q. Hamzi, A.M. Szweykowska, N.J. Leopard, K.L. Carraway, T. Fujii, J.P. Helgeson, R.N. Loeppky, Phytochemistry 6 (1967) 1169.
[2] P. Cohen, Nat. Cell Biol. 4 (2002) E127.
[3] D.O. Morgan, Nat. Cell Biol. 4 (2002) E127.
[4] R.I. Pennel, C. Lamb, Plant Cell 9 (1997) 1157.
[5] Y. Katakura, Biosci. Biotechnol. Biochem. 70 (2006) 1076.
[6] C.A. Schmidt, Biochim. Biophys. Acta-Rev. Cancer 1775 (2007) 5.
[7] T.M. Sielecki, J.F. Boylan, P.A. Benfield, G.L. Trainor, J. Med. Chem. 43 (2000) 1.
[8] P. Cohen, Nat. Rev. Drug Discov. 1 (2002) 309.
[9] P.S. Sharma, R. Sharma, R. Tyagi, Curr. Cancer Drug Tar. 8 (2008) 53.
[10] M. Legraverend, O. Ludwig, E. Bisagni, S. Leclerc, L. Meijer, Bioorg. Med. Chem. Lett. 8 (1998) 793.
[11] M. Legraverend, P. Tunnah, M. Noble, P. Ducrot, O. Ludwig, D.S. Grierson, M. Leost, L. Meijer, J. Endicott, J. Med. Chem. 43 (2000) 1282.
[12] F.I. Raynaud, S.R. Whittaker, P.M. Fischer, S. McClue, M.I. Walton, S.E. Barrie, M.D. Garrett, P. Rogers, S.J. Clarke, L.R. Kelland, M. Valenti, L. Brunton, S. Eccles, D.P. Lane, P. Workman, Clin. Cancer Res. 11 (2005) 4875.
[13] A.Y. Louye, T.J. Meade, Chem. Rev. 99 (1999) 2711.
[14] H. Sigel, Chem. Soc. Rev. 33 (2004) 191.
[15] R. Olar, M. Badea, D. Marinescu, C.M. Chifiriuc, C. Bleotu, M.N. Grecu, E.E. Iorgulescu, M. Bucur, V. Lazar, A. Finaru, Eur. J. Med. Chem. 45 (2010) 2868.
[16] P. Štarha, I. Popa, Z. Trávníček, Inorg. Chim. Acta 363 (2010) 1469.
[17] H.H. Hammud, G. Nemer, W. Sawma, J. Touma, P. Barnabe, Y. Bou-Mouglabey, A. Ghannoum, J. El-Hajjar, J. Usta, Chem.-Biol. Interact. 173 (2008) 84.
[18] Z. Trávníček, M. Matiková-Malarová, Acta Cryst. 62 (2006) 4377.
[19] J.A. Kuhnle, G. Fuller, J. Corse, B.E. Mackey, Physiol. Plant 41 (1977) 14.
[20] M.W. Bullock, J.J. Hand, E.L.R. Stokstad, J. Am. Chem. Soc. 78 (1956) 3693.
[21] C.H. Oh, S.C. Lee, K.S. Lee, E.R. Woo, C.Y. Hong, B.S. Yang, D.J. Baek, J.H. Cho, Arch. Pharm. Pharm. Med. Chem. 332 (1999) 187.
[22] G.M. Sheldrick, Acta Crystallogr. A 64 (2008) 112.
[23] Brandenburg, K. DIAMOND. Release 3.2d. Crystal Impact GbR, Bonn, Germany, 2006.
[24] T. Janowski, P. Pulay, Chem. Phys. Lett. 447 (2007) 27.
[25] M. Feyereisen, G. Fitzgerald, A. Komornicki, Chem. Phys. Lett. 208 (1993) 359.
[26] P. Jurečka, P. Nachtigall, P. Hobza, Phys. Chem. Chem. Phys. 3 (2001) 4578.
[27] J. Braun, H.J. Neusser, P. Hobza, J. Phys. Chem. A 107 (2003) 3918.
[28] Gaussian 03, Revision C.02, M.J. Frisch, G.W. Trucks, H.B. Schlegel, G.E. Scuseria, M.A. Robb, J.R. Cheeseman, J.A. Montgomery, Jr., T. Vreven, K.N. Kudin, J.C. Burant, J.M. Millam, S.S. Iyengar, J. Tomasi, V. Barone, B. Mennucci, M. Cossi, G. Scalmani, N. Rega, G.A. Petersson, H. Nakatsuji, M. Hada, M. Ehara, K. Toyota, R. Fukuda, J. Hasegawa, M. Ishida, T. Nakajima, Y. Honda, O. Kitao, H. Nakai, M. Klene, X. Li, J.E. Knox, H.P. Hratchian, J.B. Cross, V. Bakken, C. Adamo, J. Jaramillo, R. Gomperts, R.E. Stratmann, O. Yazyev, A.J. Austin, R. Cammi, C. Pomelli, J.W. Ochterski, P.Y. Ayala, K. Morokuma, G.A. Voth, P. Salvador, J.J. Dannenberg, V.G. Zakrzewski, S. Dapprich, A.D. Daniels, M.C. Strain, O. Farkas, D.K. Malick, A.D. Rabuck, K. Raghavachari, J.B. Foresman, J.V. Ortiz, Q. Cui, A.G. Baboul, S. Clifford, J. Cioslowski, B.B. Stefanov, G. Liu, A. Liashenko, P. Piskorz, I. Komaromi, R.L. Martin, D.J. Fox, T. Keith, M.A. Al-Laham, C.Y. Peng, A. Nanayakkara, M. Challacombe, P.M.W. Gill, B. Johnson, W. Chen, M.W. Wong, C. Gonzalez, J.A. Pople, Gaussian, Inc., Wallingford, CT, 2004.
[29] R. Ahlrichs, M. Bär, M. Häser, H. Horn, C. Kölmel, Chem. Phys. Lett. 162 (1989) 165.
[30] P. Sinha, S.E. Boesch, C. Gu, R.A. Wheeler, A.K. Wilson, J. Phys. Chem. A 108 (2004) 9213.
[31] B. Brauer, R.B. Gerber, M. Kabeláč, P. Hobza, J.M. Bakker, A.G.A. Riziq, M.S. de Vries, J. Phys. Chem. A 109 (2005) 6974.
[32] C.J. Pouchert, The Aldrich Library of Infrared Spectra, Aldrich Chemical Company Press, Milwaukee, 1981.
[33] K. Nakamoto, Infrared and Raman Spectra of Inorganic and Coordination Compounds Part B: Applications in Coordination, Organometallic and Bioinorganic Chemistry, Wiley, New York, 1991.
[34] Z. Dhaouadi, M. Ghomi, J.C. Austin, R.B. Girling, R.E. Hester, P. Mojzes, L. Chinski, P.Y. Turpin, C. Coulombeau, H. Jobic, J. Tomkinson, J. Phys. Chem. 97 (1993) 1074.
[35] M. Majoube, P. Millié, L. Chinski, P.I. Turpin, G. Vergoten, J. Mol. Struct. 355 (1995) 147.
[36] H. Poel, G. Koten, K. Vrieze, Inorg. Chem. 19 (1980) 1145.